Color Transparency at COMPASS via Exclusive Coherent Vector Meson Production [1]

Murray Moinester[2], Oleg A. Grajek[3], Eli Piasetzky[2], Andrzej Sandacz[3]

[2] School of Physics and Astronomy, R. and B. Sackler Faculty of Exact Sciences, Tel Aviv University, 69978 Ramat Aviv, Israel

[3] Sołtan Institute for Nuclear Studies, ul. Hoża 69, PL 00-681 Warsaw, Poland,

E-mails: murraym@tauphy.tau.ac.il, oleg@fuw.edu.pl, eip@tauphy.tau.ac.il, sandacz@fuw.edu.pl

Abstract

We examine the potential of the COMPASS experiment at CERN to study color transparency via exclusive coherent vector meson production in hard muon-nucleus scattering. It is demonstrated that COMPASS has high sensitivity to test this important prediction of perturbative QCD.

---

[1]Talk presented at 2002 Praha Advanced Study Institute "Symmetries and Spin" Workshop, Praha-SPIN-2002, July 2002, Prague, Czech Republic. The conference www site is http://mfinger.home.cern.ch/mfinger/praha2002//.

arXiv:hep-ex/0212061v1 26 Dec 2002

1 Introduction

One of predictions of perturbative QCD (pQCD) is that at high Q^2 the longitudinally polarized virtual photons γ_L^* fluctuate into hadronic components, e.g. $q\bar{q}$ pairs, whose transverse size $b = |\,\bar{r}_{\perp q} - \bar{r}_{\perp \bar{q}}\,|$ decreases with Q^2, $b^2 \propto (1/Q^2)$. At large Q^2 the values of b are significantly smaller than the size of the nucleon. *Color transparency* (CT) is a phenomenon of pQCD, whose characteristic feature is that small color-singlet objects interact with hadrons with small cross sections [1, 2, 3]. Cross section for the interaction of such small object, or small size configuration (SSC), with a hadron target has been calculated in pQCD using the factorization theorem [4, 3, 5], as:

$$\sigma_{q\bar{q},\,N} = \frac{\pi^2}{3}\, b^2\, \alpha_s(Q^2)\, x\, g(x,\,Q^2)\,, \tag{1}$$

where $g(x,\,Q^2)$ is the gluon distribution function in the nucleon.

Observing CT in particular kinematics would prove experimentally the applicability of the pQCD factorization theorem for those kinematics. Such a proof provides important complementary support to a class of spin physics experiments, for example related to measurements of generalized parton distributions at COMPASS [6].

The prerequisite for observing CT is to select a sample containing SSC's via a hard process (i.e. with large Q^2, high p_t, or large produced mass). For hard exclusive ρ^0 leptoproduction, in addition to large Q^2, selection of the longitudinally polarized mesons is required. To probe the SSC–nucleon cross sections one should study absorption of the SSC propagating through nuclear matter. In order to clearly observe CT it is necessary that the SSC lives long enough to traverse distances larger than the size of the target nucleus, and that the SSC stays small while propagating through the nucleus. These requirements are characterized in terms of the coherence length l_c (the distance traversed by the $q\bar{q}$ fluctuation of the virtual photon in the target nucleon/nucleus system) and by the formation length (the distance in the target system after a scattering needed for the $q\bar{q}$ fluctuation to develop into a hadron).

We consider here only exclusive *coherent* vector meson V production at small $|t|$. We analysed the coherent and incoherent channels in Refs [7, 8]. For near-forward ($t \approx 0$) coherent production and complete CT, one expects that the cross section for the nuclear target is related to that for the nucleon target, provided that $|t_{\min} <R_A^2> /3| \ll 1$, by:

$$\frac{\mathrm{d}\sigma}{\mathrm{d}t}(\gamma^* A \rightarrow V A)\,|_{t\approx 0} = A^2 \frac{\mathrm{d}\sigma}{\mathrm{d}t}(\gamma^* N \rightarrow V N)\,|_{t\approx 0}\,. \tag{2}$$

Usually in experiments the t-integrated coherent cross section is measured, for which CT predicts an approximate $A^{4/3}$ dependence. Without CT, if a hadron propagates in nuclear matter, the expected A-dependence is weaker; $A^{2/3}$ for the cross sections comparable to the pion–nucleon cross section.

In searches for CT a commonly used quantity, measured in experiments, is the *nuclear transparency*

$$T = \frac{\sigma_A}{A\,\sigma_N}\,, \tag{3}$$

which is the ratio of the cross section per nucleon for a selected process on a nucleus A to the corresponding cross section on a free nucleon.

We concentrate on exclusive coherent vector meson production (EVMP), which could be studied at the COMPASS experiment [9, 10]. Kinematic variables used in this paper are listed in Table 1.

Table 1: Kinematic variables used in the text.

$k,\ k'$	four-momentum of the incident and scattered muon,
$p,\ v$	four-momentum of the target nucleon and vector meson V,
$q = k - k'$	four-momentum of the virtual photon,
$Q^2 = -q^2$	virtuality of the photon γ^*,
$\nu = (p \cdot q)/M_p$	energy of the virtual photon in the laboratory system,
	M_p is the proton mass,
$x = Q^2/(2M_p\nu)$	Bjorken scaling variable,
$t = (q - v)^2$	squared four-momentum transfer to the target,
p_t^2	transverse-momentum squared of the vector meson,
$m_V = (v^2)^{\frac{1}{2}}$	invariant mass of the vector meson V,
$M_X^2 = (p + q - v)^2$	missing-mass squared of the undetected recoiled system,
$I = (M_X^2 - M_p^2)/W^2$	inelasticity

In order to study CT for the exclusive production of mesons composed of light quarks (like ρ) one should select *large Q^2*, *moderately small x* and *longitudinally* polarized mesons.

The t-dependence of the cross section for exclusive meson production on the nucleon is approximately exponential, $e^{B(t-t_{\min})}$, where $t_{\min} \approx -M_p^2 x^2 (1 + m_V^2/Q^2)^2$ and m_V is the mass of the produced meson. For hard EVMP, if SSC's are important, the slope B significantly decreases with increasing Q^2, approaching a universal value $(4.5 - 5\ \text{GeV}^{-2})$ related to the nucleon radius. This is so because the transverse interquark distance in the SSC decreases with increasing Q^2.

For EVMP on a nucleus A the t-dependence of the cross section is approximately reproduced by a sum of two exponential functions. The peak at the lowest $|t|$ values, with the slope proportional to the nucleus radius squared, $< R_A^2 >$, is mostly due to the coherent production, whereas at somewhat larger $|t|$ the incoherent production on quasi-free nucleons dominates and the slope is almost equal to that for the production on free nucleons. Applying cuts on t allows to select successfully samples of events, which are strongly dominated by either coherent or incoherent production, as discussed in Refs. [11, 12, 13].

Strong recent evidence for CT comes from Fermilab E791 experiment on the A-dependence of coherent diffractive dissociation of pions into two high-p_t jets [13]. Also the E691 experiment results on A-dependence of coherent J/ψ photoproduction [12] and the NMC measurements of A-dependence of coherent and quasielastic J/ψ muoproduction are *consistent* with CT, but don't demonstrate it unambiguously.

2   Experimental method

We proposed [7] to study CT via *exclusive coherent ρ meson production $\mu A \to \mu\,\rho A$* on C and Pb nuclei, as well as the exclusive production of other vector mesons. The preferable decay modes are those into the charged particles such as $\rho^0 \to \pi^+\pi^-$.

We propose to complement the initial setup of the COMPASS [9, 10] for the muon-beam run with the polarized target by adding the nuclear targets downstream of the polarized target.

The high-intensity high-energy incident muon-beam will impinge on the polarized target and a downstream thin nuclear target. The momenta of the scattered muon and of

the produced charged particles will be reconstructed in the two magnetic spectrometers, using the magnets SM1 and SM2, instrumented with various tracking detectors. In order to select exclusive events, we rely only on the kinematics of the scattered muon and the produced meson.

The trigger will use the information from hodoscopes registering the scattered muons, and from calorimeters registering deposits of energy of the particles in the final state.

The discrimination of non-exclusive events will be done by applying cuts on the inelasticity I (for the definition see Table 1). In Fig. 1 the inelasticity distribution is shown for the SMC ρ^0 sample [14] for the events with the invariant mass in the central part of the ρ^0 peak. For the inelasticity distribution the peak at $I = 0$ is the signal of exclusive ρ^0 production. Non-exclusive events, where in addition to detected fast hadrons, slow undetected hadrons were produced, appear at $I > 0$. With larger statistic in COMPASS it will be possible to apply more tight inelasticity cuts in order to further reduce the background.

The selections of coherent or incoherent production will be done on a statistical basis, using the t-distribution; at the lowest $|t|$ values coherent events predominate.

Separation of the ρ^0 samples with the enhanced content of longitudinally or transversely polarized mesons will be done by applying cuts on the measured angular distributions of pions from the decays of the parent ρ^0.

The minimal covered Q^2-range is expected to be $0.05 < Q^2 < 10\,\mathrm{GeV}^2$. For the medium and large Q^2 values ($Q^2 > 2\,\mathrm{GeV}^2$) the range $0.006 < x < 0.1$ will be covered with good acceptance.

The basic observable for each process studied will be the ratio of the nuclear transparencies for lead and carbon, $R_\mathrm{T} = T_\mathrm{Pb}/T_\mathrm{C} = (\sigma_\mathrm{Pb}/A_\mathrm{Pb})/(\sigma_\mathrm{C}/A_\mathrm{C})$.

3   Simulation of exclusive ρ^0 events

We present details of the simulation of exclusive coherent ρ^0 production ($\mu A \to \mu\,\rho^0 A$) in the COMPASS experiment with the carbon and lead targets. The simulations were done with a dedicated fast Monte Carlo program which generates deep inelastic exclusive ρ^0 events with subsequent decay $\rho^0 \to \pi^+\pi^-$. At this stage there was no attempt to include any background in the event generators. Details of the used parameterization of the cross section for the production of ρ^0 on the free nucleon, $\mu N \to \mu\,\rho^0 N$, with the subsequent decay $\rho^0 \to \pi^+\pi^-$ were presented in Ref. [7]. We relate the differential cross sections for the free nucleon to these for coherent production on the nucleus A via

$$\left(\frac{\mathrm{d}\sigma_A^{\mathrm{coh}}}{\mathrm{d}t}\right)_i = A_{\mathrm{eff,\ coh}}^2 \cdot e^{<R_A^2> t/3} \cdot \left(\frac{\mathrm{d}\sigma_N}{\mathrm{d}t}\right)_i . \tag{4}$$

Here $<R_A^2>$ is the mean squared radius of the nucleus, $A_{\mathrm{eff,\ coh}}$ takes account of nuclear screening for the coherent process, and $i = L$ or T designates the polarization of ρ^0. We used the approximation $t - t_{min} \simeq -p_t^2$.

We generated the cross sections for two models. For the complete color transparency model (CT model) we used $A_{\mathrm{eff,\ coh}} = A$. In another model we assumed a substantial nuclear absorption (NA model) and used $A_{\mathrm{eff,\ coh}} = A^{0.75}$.

Details of the simulation of the apparatus effects were given in [7]. Here we discuss only the trigger simulation. To simulate the trigger acceptance a trajectory of the scattered muon behind the second magnet was calculated, and the hits in the muon hodoscopes were checked. We consider two different trigger acceptances, the Medium Q^2 range Trigger

(MT) and the Full Q^2 range Trigger (FT). The Q^2-dependence of the trigger efficiency is denoted ϵ_{tr}. For the MT trigger at 190 GeV beam, ϵ_{tr} decreases quickly with Q^2 from 0.7 at $Q^2 = 2\,\mathrm{GeV}^2$ to about 0.1 at $Q^2 = 10\,\mathrm{GeV}^2$. For the FT trigger the Q^2-dependence is weaker and the trigger acceptance is higher; it is always bigger than 0.5 for $Q^2 < 70\,\mathrm{GeV}^2$ at 190 GeV beam energy.

4   Results on exclusive ρ^0 production

We considered 190 GeV muon beam. The simulations were done independently for the carbon ($A = 12$) and lead targets ($A = 207$), and for two triggers (MT and FT). For each target and each trigger we assumed two different models describing the nuclear effects for exclusive ρ^0 production: CT model and NA model (cf. Section 3).

The kinematic range considered was the following:

$$2 < Q^2 < 80\,\mathrm{GeV}^2 \,, \tag{5}$$

$$35 < \nu < 170\,\mathrm{GeV} \,. \tag{6}$$

The upper cut on ν was chosen to eliminate the kinematic region where the amount of radiative events is large, whereas the lower one to eliminate the region where the acceptance for pions from ρ^0 decay is low.

The total efficiency ϵ_{tot} to observe exclusive ρ^0 events results from: the acceptance of the trigger (ϵ_{tr}), acceptance to detect the pions (ϵ_{had}), efficiency for tracks reconstruction (ϵ_{rec}), cut on the invariant mass of two pions, $0.62 < M_{\pi\pi} < 0.92$ GeV, used for the selection of the samples (ϵ_{mass}), and efficiency for an event to survive the secondary interactions (ϵ_{sec}). The contributions of all these effects to ϵ_{tot} are similar to those presented in [15] for the polarized target, except for the effects of the secondary interactions. The approximate value of ϵ_{sec} is equal to 0.87 for the carbon target and 0.94 for the lead target. The total efficiency ϵ_{tot} is about 0.48 for the FT trigger and about 0.30 for the MT trigger.

The total expected cross section for exclusive ρ^0 production on the nucleon is

$$\sigma_{\mu N \to \mu \rho^0 N}^{\mathrm{tot}} = \int_{\nu_{\mathrm{min}}}^{\nu_{\mathrm{max}}} \int_{Q_{\mathrm{min}}^2}^{Q_{\mathrm{max}}^2} \sigma_{\mu N \to \mu \rho^0 N}(Q^2,\,\nu)\,\mathrm{d}Q^2\,\mathrm{d}\nu \,, \tag{7}$$

where the kinematic range was defined before. The value of $\sigma_{\mu N \to \mu \rho^0 N}^{\mathrm{tot}}$ is 283 pb. For nuclear targets the corresponding values depend on A and on the assumed model for nuclear absorption.

The expected muon beam intensity will be about 10^8/s during spills of length of about 2 s, which will repeat every 14.4 s. With the proposed thin nuclear targets, each of 17.6 g/cm^2, the luminosity will be $\mathcal{L} = 12.6\,\mathrm{pb}^{-1} \cdot \mathrm{day}^{-1}$. The estimates of the numbers of accepted events were done for a period of data taking of 150 days (1 year), divided equally between two targets. An overall SPS and COMPASS efficiency of 25% was assumed. The numbers of accepted events for the carbon and lead targets, assuming the two models for the nuclear absorption mentioned earlier, are given in Table 2.

The distributions of accepted exclusive events as a function of x, Q^2 and ν are similar to those presented in [15].

In Fig. 2 we present the p_t^2 distributions for both targets. We observe clear coherent peaks at small p_t^2 ($< 0.05\,\mathrm{GeV}^2$) and less steep distributions for the incoherent events at larger p_t^2. The arrows at the top histograms indicate the cut $p_t^2 > 0.1\,\mathrm{GeV}^2$, used to select

Table 2: Numbers of accepted events for two considered models of the nuclear absorption.

model	N_{C}	N_{Pb}
CT	70 000	200 000
NA	28 000	20 000

the incoherent samples. For the middle and bottom histograms the arrows indicate the cut $p_t^2 < 0.02\,\mathrm{GeV}^2$, used to select the samples which are dominated by coherent events — the so called coherent samples. For the samples defined by the latter cut the fraction of the incoherent events is at the level of up to 10%, depending on the nucleus and on the model for nuclear absorption.

The effect of the kinematical smearing on p_t^2 may be seen by comparing the distributions for the generated events (middle row) to the ones for measured events (bottom row) where the acceptance and smearing were included. The smearing of p_t^2 increases with increasing p_t^2; it is about $0.006\,\mathrm{GeV}^2$ for the coherent samples ($p_t^2 < 0.02\,\mathrm{GeV}^2$) and about $0.03\,\mathrm{GeV}^2$ for the incoherent samples ($p_t^2 > 0.1\,\mathrm{GeV}^2$).

The analysis of the ρ^0 decay distributions allows us to study spin-dependent properties of the production process [16], in particular the polarization of ρ^0. The ρ^0 decay angular distribution $W(\cos\theta, \phi)$ is studied in the s-channel helicity frame. The ρ^0 direction in the virtual photon–nucleon centre-of-mass system is taken as the quantization axis. The angle θ is the polar angle and ϕ the azimuthal angle of the π^+ in the ρ^0 rest frame. The $\cos\theta$ distributions for pions from ρ^0 decays are shown in Fig. 3 for the lead target. The distributions for longitudinally (dashed lines) and transversely (dotted lines) polarized parent ρ^0's are markedly different. Their sum is also indicated.

As Q^2 increases, the approach to the CT limit is expected to be different for EVMP by longitudinally polarized virtual photons from that by transversely polarized photons. To increase the sensitivity of the search for CT, we study A-dependence of the cross sections for samples with different ρ^0 polarizations, which will be selected by cuts on $\cos\theta$. Such cuts will allow us to select the samples with enhanced contributions of the events initiated by the virtual photons of a desired polarization. Studies of the samples with *different polarizations* of the virtual photons are *necessary* for the unambiguous demonstration of CT.

Another aspect which is important for CT studies, is the covered range of the coherence length l_c (cf. Section 1). We showed in Ref. [7] the correlation of l_c vs. Q^2 for a sample of accepted events. At small l_c values the effects of initial and final state interactions in the nuclei mimic CT [17]. It is important to disentangle effects due to CT from those caused by the modified absorption at small l_c values.

For a limited statistics, we may use the combined data at l_c values exceeding the sizes of the target nuclei. The radius of the carbon nucleus is $< r_{\mathrm{C}}^2 >^{1/2} = 2.5$ fm and that of the lead nucleus is $< r_{\mathrm{Pb}}^2 >^{1/2} = 5.5$ fm. Therefore, one may use the selection $l_c > l_c^{\min} \simeq 2 \cdot < r_{\mathrm{Pb}}^2 >^{1/2} = 11$ fm. About a half of events survive such a cut on l_c. These events cover the range of $Q^2 < 6\,\mathrm{GeV}^2$, which is expected to be sufficient to observe CT.

The estimated values and statistical precision of R_{T}, the ratio of the nuclear transparencies for lead and carbon, are presented for different Q^2 bins in Fig. 4 for $p_t^2 < 0.02\mathrm{GeV}^2$. The Q^2 bins are specified in Table 3. Figure 4 comprises predictions for two models, CT

6

Table 3: Q^2 bins used for the determination of R_{T}.

Bin number	Q^2 bin [GeV^2]	$< Q^2 >$ [GeV^2]	$< x >$
1	2–3	2.4	0.016
2	3–4	3.4	0.022
3	4–6	4.8	0.031
4	6–9	7.2	0.048
5	9–12	10.2	0.072
6	12–20	14.8	0.11

and NA, and for 6 different samples of accepted events for each model. For each sample a set of "measurements" in different Q^2 bins is shown. Sets **A** and **B** were obtained using the standard selections for the MT and FT triggers, respectively. Four remaining sets were obtained for the FT trigger with additional selections: **C** with $|\cos\theta| < 0.4$, **D** with $|\cos\theta| > 0.7$, **E** with $|\cos\theta| < 0.4$ and $l_c > 11$ fm, and **F** with $|\cos\theta| > 0.7$ and $l_c > 11$ fm. Note that for sets **E** and **F** only three lower Q^2 bins appear. One expects large differences in R_{T} for the two considered models. For coherent samples $R_{\mathrm{T}} \approx 5$ for CT model and ≈ 1 for NA model. At $Q^2 \simeq 5\,\mathrm{GeV}^2$ the precision of the measurement of R_{T} for coherent events will be better than 17%, even for the restricted samples **E** and **F**, thus allowing excellent discrimination between the two models for the nuclear absorption.

5 Comparison with previous experiments

We compare COMPASS capabilities to demonstrate CT to those of previous experiments in which exclusive coherent ρ^0 leptoproduction on nuclear targets was studied. For the comparison we must also select experiments which covered Q^2 range extending to large values, bigger than 2 GeV^2. The only experiment which published such high Q^2 exclusive coherent data is the NMC experiment [18].

NMC has published data on coherent exclusive ρ^0 production on ^{2}H, C and Ca targets. The muon beam energy was 200 GeV and the data cover the ranges $2 < Q^2 < 25\,\mathrm{GeV}^2$ and $1 < l_c < 30$ fm. Due to the moderate statistics of the data the Q^2-dependence of nuclear absorption was not obtained at sufficiently large or at fixed l_c, which is necessary to unambiguously demonstrate CT.

The COMPASS data at medium and large Q^2 (FT trigger) will cover the kinematic range similar to that of the NMC data. The expected statistics for the carbon target will be about 2 orders of magnitude higher than that of the NMC data for the same target. This increase is in particular due to higher beam intensity and larger acceptance in the COMPASS experiment. In addition COMPASS will use also lead target and will extend measurements to small Q^2. Due to large statistics splitting of COMPASS data in several Q^2 and l_c bins as well as the selection of events with longitudinal or transverese ρ^0 polarization

will be possible.

6 Conclusions

We have simulated and analysed exclusive ρ^0 muoproduction at the COMPASS experiment using thin nuclear targets of carbon and lead. For muon beam energy of 190 GeV and a trigger for medium and large Q^2, the covered kinematic range is $2 < Q^2 < 20\,\mathrm{GeV}^2$ and $35 < \nu < 170\,\mathrm{GeV}$.

Good resolutions in Q^2, l_c, t (p_t^2) and $\cos\theta$ are feasible. An efficient selection of coherent events is possible by applying cuts on p_t^2. In order to obtain the samples of events initiated with a probability of about 80% by either γ_L^* or γ_T^*, the cuts on the ρ^0 decay angular distribution of $\cos\theta$ will be used. The search for CT could be facilitated by using the events with l_c values exceeding the sizes of the target nuclei. The fraction of such events is substantial and the covered Q^2 range seems sufficient to observe CT.

We showed high sensitivity of the measured ratio R_T of nuclear transparencies for lead and carbon for different models of nuclear absorption. Good statistical accuracy of the measured R_T may be achieved already for one year of data taking. These measurements, taken at different Q^2 intervals, may allow to discriminate between different mechanisms of the interaction of the hadronic components of the virtual photon with the nucleus.

In conclusion, the planned comprehensive studies of exclusive vector meson production on different nuclear targets at the COMPASS experiment are able to unambiguously demonstrate CT.

7 Acknowledgements

References

[1] F.E. Low, Phys. Rev. **D 12** (1975) 163.

[2] S.J. Brodsky, L.L. Frankfurt, J.F. Gunion, A.H. Mueller, M.I. Strikman, Phys. Rev. **D 50** (1994) 3134.

[3] L.L. Frankfurt, G.A. Miller and M.I. Strikman, Phys. Lett. **B304** (1993) 1; Ann. Rev. Nucl. Part. Phys. **44** (1994) 501.

[4] B. Blättel, G. Baym, L.L. Frankfurt and M.I. Strikman, Phys. Rev. Lett. **70** (1993) 896.

[5] L.L. Frankfurt, A.V. Radyushkin and M.I. Strikman, Phys. Rev. **D55** (1997) 98.

[6] J. Pochodzalla, L. Mankiewicz, M. Moinester, G. Piller, A. Sandacz, M. Vander-haeghen, *Exclusive Meson Production at COMPASS*, hep-ph/9909534;
N. D'Hose, E. Burtin, P.A.M. Guichon, J. Marroncle, M. Moinester, J. Pochodzalla, A. Sandacz, *Possible Measurements of GPDs at COMPASS*, Contribution to Proceedings of the workshop "Future Physics at COMPASS", Sept. 26-27, 2002,
http://compass-cw2002.web.cern.ch/compass-cw2002/default.htm

[7] A. Sandacz, O. A. Grajek, M. Moinester, E. Piasetzky, *Color Transparency at COM-PASS*, hep-ex/0106076.

[8] M. Moinester, O. A. Grajek, E. Piasetzky, A. Sandacz, Nucl. Phys. B (Proc. Suppl.) **105** (2001) 168.

[9] G. Baum *et al*, *COMPASS. A Proposal for a Common Muon and Proton Apparatus for Structure and Spectroscopy*,
CERN/SPSLC/96-14, SPSC/P 297 (1996) and CERN/SPSLC 96-30 (1996),
http://wwwcompass.cern.ch/compass/proposal/welcome.html.

[10] F. Bradamante, Prog. Part. Nucl. Phys. **44** (2000) 339.

[11] NMC, P. Amaudruz *et al*, Nucl. Phys. **B371** (1992) 553;
NMC, M. Arneodo *et al*, Phys. Lett. **B332** (1994) 195.

[12] M.D. Sokoloff *et al*, Phys. Rev. Lett. **57** (1986) 3003.

[13] E791 Collab., E.M. Aitala *et al*, Phys. Rev. Lett. **86** (2001) 4768, 4773.

[14] A. Tripet, Nucl. Phys. B (Proc. Suppl.) **79** (1999) 529.

[15] A. Sandacz, *Hard Exclusive Meson Production at COMPASS*, COMPASS Note 2000-1,
http://wwwcompass.cern.ch/compass/notes.

[16] K. Schilling and G. Wolf, Nucl. Phys. **B61** (1973) 381.

[17] HERMES Collab., K. Ackerstaff *et al*, Phys. Rev. Lett. **82** (1999) 3025.

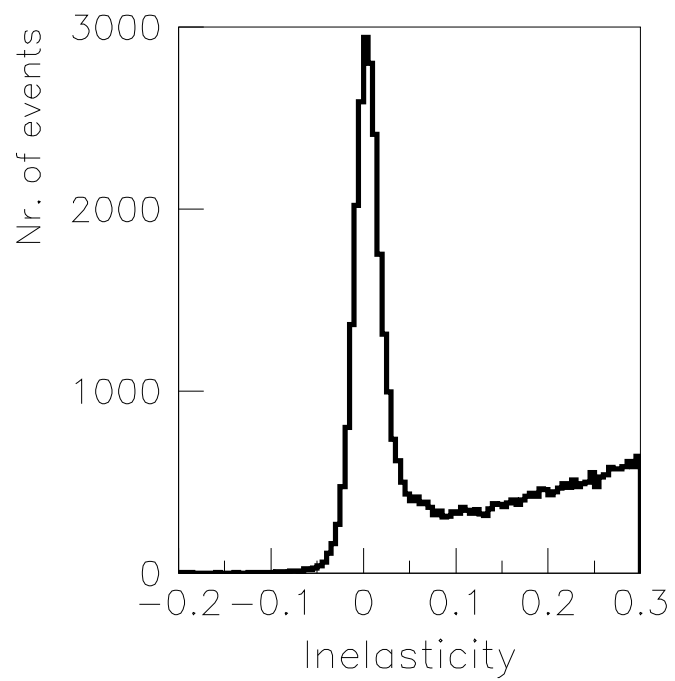[18] NMC, M. Arneodo *et al*, Nucl. Phys. **B429** (1994) 503.

Figure 1: Inelasticity distribution. The SMC preliminary results [14] for $\mu N \rightarrow \mu \rho^0 N$.
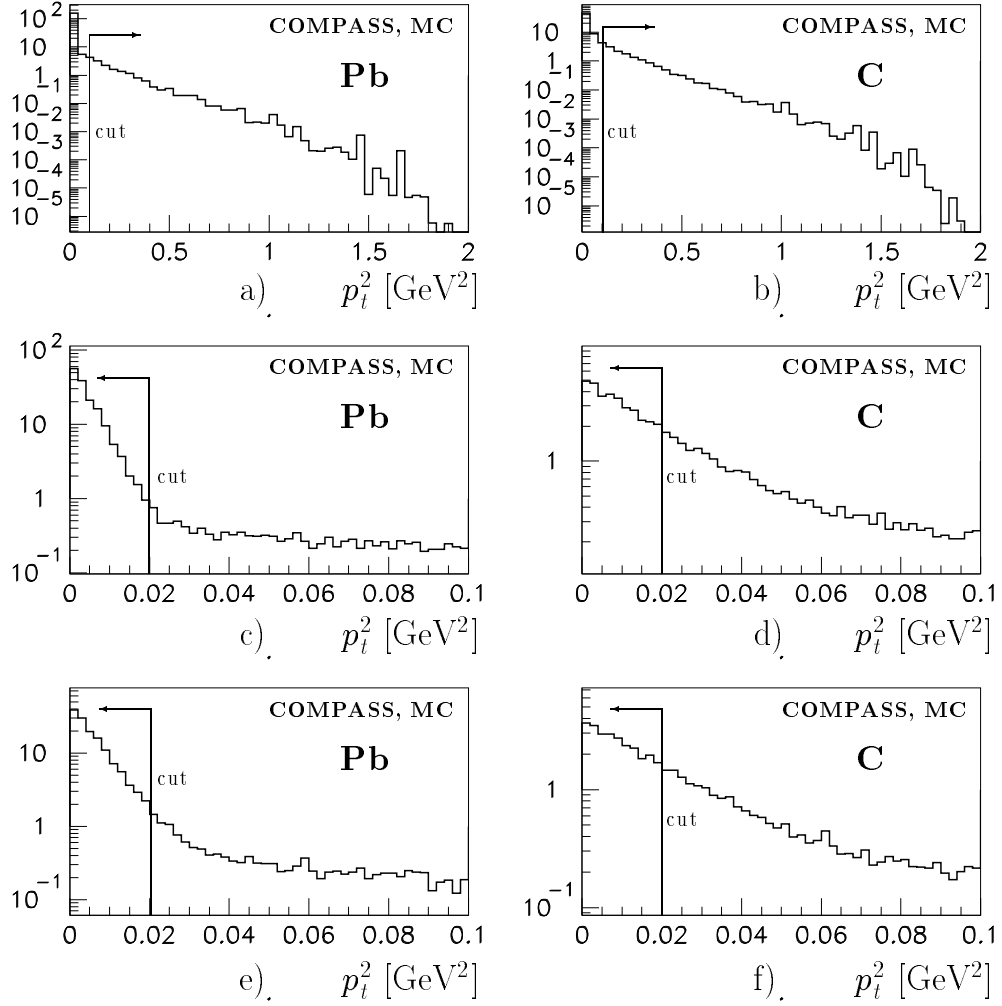
Figure 2: Distributions of p_t^2 for the lead (left) and carbon (right) targets. The distributions a) and b) at the top are for the generated events and the wide range of p_t^2, whereas those in the middle, c) and d), correspond to the range of low p_t^2. The bottom distributions, e) and f), are for the accepted events, with the kinematical smearing taken into account. The arrows show the cuts described in the text.
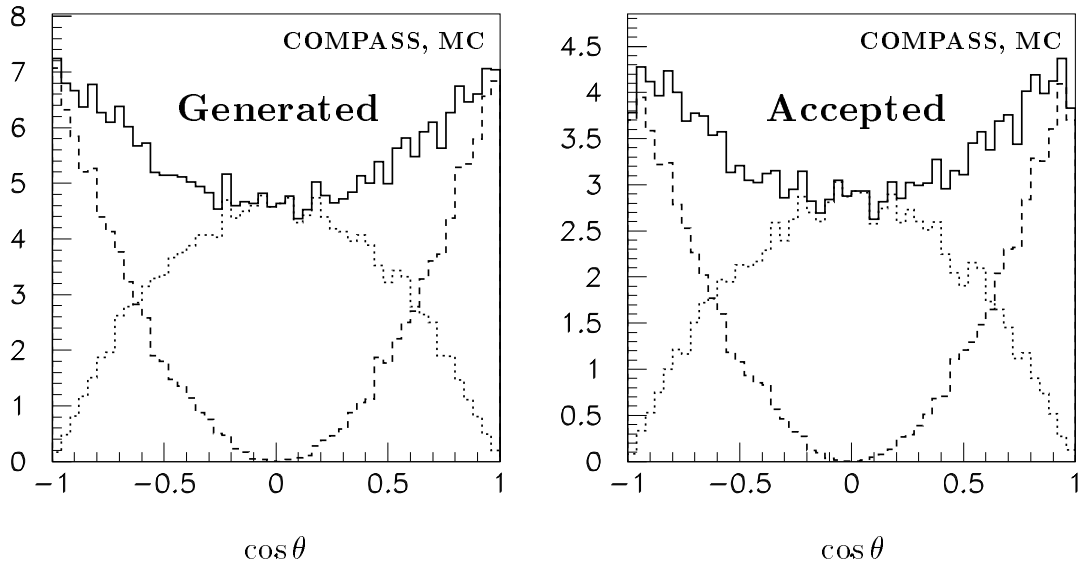
Figure 3: Distributions of $\cos\theta$ for the pions (π^+) from the decays of ρ^0 mesons produced on lead, for generated (left) and accepted (right) events. For the latter ones the effects of the kinematical smearing were taken into account. The dashed- and dotted-line histograms are for the longitudinally and transversely polarized ρ^0's, respectively, and the solid-line histograms are for their sum.
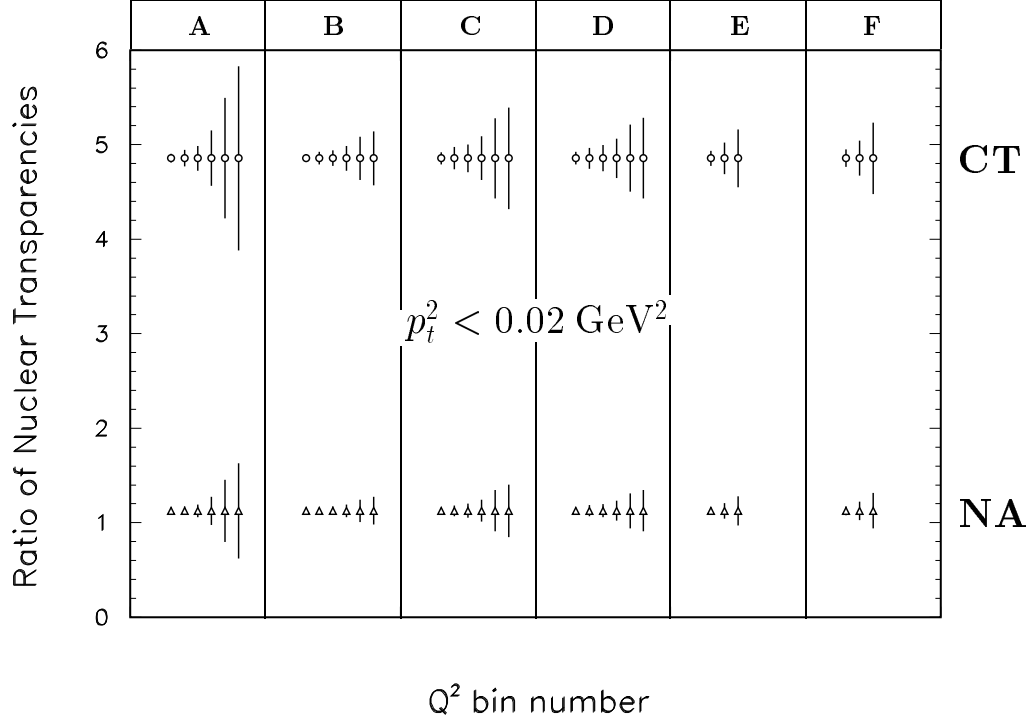
$p_t^2 < 0.02\,\mathrm{GeV}^2$

set	conditions
A	MT
B	FT
C	FT $+$ $\mid\cos\theta\mid < 0.4$
D	FT $+$ $\mid\cos\theta\mid > 0.7$
E	FT $+$ $\mid\cos\theta\mid < 0.4$ $+$ $l_c > 11\,\mathrm{fm}$
F	FT $+$ $\mid\cos\theta\mid > 0.7$ $+$ $l_c > 11\,\mathrm{fm}$

Figure 4: Expected statistical precision of the measurement of the ratio R_T of GeV^2 nuclear transparencies for lead and carbon for $p_t^2 < 0.02\,\mathrm{GeV}^2$ and for different Q^2 bins, for CT (upper band) and for NA (lower band) models. The Q^2 bins are defined in Table 3. Sets A, B, C, D, E and F correspond to the conditions specified in the table below the plot.